

Sustained Expression of Early Growth Response Protein-1 Blocks Angiogenesis and Tumor Growth

Markus Lucerna,¹ Jiri Pomyje,¹ Diana Mechtcheriakova,¹ Alexandra Kadl,¹ Florian Gruber,^{1,2} Martin Bilban,^{3,4} Yuri Sobanov,¹ Gernot Schabbauer,¹ Johannes Breuss,¹ Oswald Wagner,^{3,4} Markus Bischoff,⁵ Matthias Clauss,⁵ Bernd R. Binder,¹ and Erhard Hofer¹

Departments of ¹Vascular Biology and Thrombosis Research and ²Dermatology, ³Clinical Department of Medical and Chemical Laboratory Diagnostics, ⁴Ludwig Boltzmann Institute for Clinical and Experimental Oncology, Medical University of Vienna, Vienna, Austria and ⁵Department of Cellular and Integrative Physiology, Indiana Center of Vascular Biology and Medicine, Indianapolis

Abstract

Transient induction of the transcription factor early growth response protein-1 (EGR-1) plays a pivotal role in the transcriptional response of endothelial cells to the angiogenic growth factors vascular endothelial growth factor (VEGF) and basic fibroblast growth factor (bFGF), which are produced by most tumors and are involved in the angiogenic switch. We report here that sustained expression of EGR-1 by recombinant adenoviruses in endothelial cells, however, leads to the specific induction of potent feedback inhibitory mechanisms, including strong up-regulation of transcriptional repressors, negative cell cycle check point effectors, proteins with established antiangiogenic activity, and several proapoptotic genes. Sustained EGR-1 expression consistently leads to an antiangiogenic state characterized by an altered responsiveness to VEGF and bFGF and a striking inhibition of sprouting and tubule formation *in vitro*. Furthermore, EGR-1-expressing viruses potently inhibit cell invasion and vessel formation in the murine Matrigel model and repress tumor growth in a murine fibrosarcoma model. We propose that gene therapy involving sustained EGR-1 expression may constitute a novel therapeutic principle in the treatment of cancer due to the simultaneous induction of multiple pathways of antiangiogenesis, growth arrest, and apoptosis induction in proliferating cells leading to preferential inhibition of angiogenesis and tumor growth. (Cancer Res 2006; 66(13): 6708-13)

Introduction

Angiogenesis, the formation of new capillaries from existing vessels, is essential for tumor growth and metastasis (1, 2). Antiangiogenesis therapies, which interfere with activation of growth factor receptors, such as vascular endothelial growth factor (VEGF) receptor (VEGFR)-2 (Flk-1/KDR) or basic fibroblast growth factor

(bFGF) receptor, are functional in animal tumor models and as combination therapies in clinical studies (3). However, due to the multitude of factors produced by tumors and the genetic instability observed during cancer progression, current clinical results are lagging behind expectations. Strategies based on gene therapy interfering with pathways commonly used by different angiogenic inducers could therefore be of advantage.

One factor involved in responses to many different growth factors and environmental stresses, such as hypoxia, is early growth response protein-1 (EGR-1). It is a broadly expressed member of the Cys2-His2 zinc finger family of transcription factors and was first discovered as an immediate early gene induced in growth-quiescent fibroblasts exposed to serum (4). EGR-1 binds to GC-rich, *cis*-acting promoter elements and controls the expression of a wide variety of pathogenesis-relevant genes, including growth factors, cytokines, receptors, and proteases, many of which are involved in angiogenesis and tumorigenesis (5, 6), the response to ischemia (7) and the progress of several vascular diseases (8). EGR-1 activity is negatively controlled by the corepressor NAB2 (9), and the importance of a transient activation of EGR-1 for VEGF- and bFGF-mediated gene regulation and angiogenesis has been shown using DNazyme for EGR-1 suppression (5) or NAB2 overexpression by our group (6).

Based on the observation that, during the latter phases of transient growth factor-mediated induction, EGR-1 expression can lead to strong up-regulation of the corepressor NAB2 (Table 1; ref. 6) and other molecules with the potential to limit proangiogenic responses in a negative feedback loop, we have now investigated to what extent this phenomenon could be exploited to induce an antiangiogenic state in endothelial cells. We have therefore analyzed the influence of sustained adenoviral overexpression of EGR-1 on gene expression in endothelial cells, angiogenesis, and tumor growth.

Materials and Methods

Cell culture. Human umbilical vascular endothelial cells (HUVEC), human uterine microvascular endothelial cells (HUMEC), and MethA fibrosarcoma cells were prepared and cultured as described previously (6, 10). Cells were induced with 50 ng/mL recombinant human VEGF165 or bFGF (PromoCell, Heidelberg, Germany).

Recombinant adenoviral constructs and infection. The coding region of the human *EGR-1* gene, including the single intron, was amplified from the PAC clone E13873Q3 (library no. 704, Deutsches Ressourcenzentrum für Genomforschung GmbH, Berlin-Charlottenburg, Germany) by PCR and subcloned into the pACCMVpASR+ vector (6). EGR-1-expressing viruses (Ad.EGR-1) were obtained by homologous recombination as described (6). NAB2- and NAB2.as-expressing viruses (Ad.NAB2 and Ad.NAB2.as), an empty control virus (Ad.con), and a control virus expressing green fluorescent protein (GFP; Ad.GFP) have been reported previously (6). Adenovirus

Note: Supplementary data for this article are available at Cancer Research Online (<http://cancerres.aacrjournals.org>).

Current address for M. Lucerna: Division of Biopharmaceutics, Leiden/Amsterdam Center for Drug Research, Leiden University, Einsteinweg 55, NL-2333 Leiden, the Netherlands.

Current address for D. Mechtcheriakova and Y. Sobanov: Novartis Research Institute, Brunnerstrasse 59, A-1230 Vienna, Austria.

Current address for A. Kadl: Cardiovascular Research Center, University of Virginia, P.O. Box 801394, Charlottesville, VA 22908.

Requests for reprints: Erhard Hofer, Department of Vascular Biology and Thrombosis Research, Center of Biomolecular Medicine and Pharmacology, Medical University of Vienna, Vienna Competence Center, Lazarettgasse 19, A-1235 Vienna, Austria. Phone: 43-1-40160-33111; Fax: 43-1-40160-933100; E-mail: erhard.hofer@meduniwien.ac.at.

©2006 American Association for Cancer Research.
doi:10.1158/0008-5472.CAN-05-2732

Table 1. Selected genes up-regulated or down-regulated by sustained EGR-1 expression as delineated from Affymetrix microarray analysis

UniGene ID	Entrez gene	Gene symbol	Entrez definition	EGR-1 (16 h)	Control virus (16 h)	EGR-1 (24 h)	Control virus (24 h)	EGR-1 (48 h)	Control virus (48 h)
Transcriptional repression/modulation									
Hs.159223	4665	<i>NAB2</i>	<i>NGFI-A -binding protein 2 (EGR-1-binding protein 2)</i>	4.5	-0.3	4.1	0	3.8	-0.4
Hs.107474	4664	<i>NAB1</i>	<i>NGFI-A -binding protein 1 (EGR-1-binding protein 1)</i>	2.9	0.2	3.1	0.1	3.0	0.8
Hs.25292	3726	<i>JUNB</i>	<i>Jun B proto-oncogene</i>	2.6	-0.2	2.8	-0.2	3.4	0.2
Hs.2780	3727	<i>JUND</i>	<i>Jun D proto-oncogene</i>	1.9	0.4	1.7	-0.1	1.2	0.7
Antiangiogenesis									
Hs.24395	9547	<i>CXCL14</i>	<i>Chemokine (C-X-C motif) ligand 14</i>	3.8	0	8.0	0.2	11.9	0.2
Hs.446641	7076	<i>TIMP-1</i>	<i>Tissue inhibitor of metalloproteinase-1 (erythroid-potentiating activity)</i>	3	0	3.5	0.2	3.3	0.4
Hs.245188	7078	<i>TIMP-3</i>	<i>Tissue inhibitor of metalloproteinase-3 (Sorsby fundus dystrophy)</i>	1.3	-0.3	2.8	0.3	4.7	1.4
Hs.347713	2321	<i>FLT1</i>	<i>fms-related tyrosine kinase 1</i>	1.3	0.2	1.5	0.6	1.4	0.5
Hs.12337	3791	<i>KDR</i>	<i>Kinase insert domain receptor</i>	-0.7	0.2	-0.7	0.4	-2.6	0.8
Hs.77274	5328	<i>PLAU</i>	<i>Plasminogen activator, urokinase</i>	-2.1	-0.6	-1.3	-0.7	-0.8	-0.9
Cell cycle arrest									
Hs.106070	1028	<i>CDKN1C</i>	<i>Cyclin-dependent kinase inhibitor 1C (p57, Kip2)</i>	3.2	-0.3	3.8	0.2	5.8	0.4
Hs.110571	4616	<i>GADD45B</i>	<i>Growth arrest- and DNA damage-inducible, β</i>	0.1	-1.9	1.3	-1.9	4.1	-3.3
Hs.1103	7040	<i>TGF-β1</i>	<i>Transforming growth factor-β1 (Camurati-Engelmann disease)</i>	1.9	0	1.0	1.1	2.0	-0.3
Proapoptosis									
Hs.1183	1844	<i>DUSP2</i>	<i>Dual-specificity phosphatase 2</i>	4.3	0	6	0	5.8	-0.4
Hs.112058	10572	<i>SIVA</i>	<i>CD27-binding (Siva) protein</i>	1.8	0.2	2.6	-0.6	3.9	-0.1
Hs.293225	162989	<i>DEDD2</i>	<i>Death effector domain containing 2</i>	1.8	0.3	2.4	0.3	2.8	0.5
Others									
Hs.110675	348	<i>APOE</i>	<i>Apolipoprotein E</i>	7.4	-0.2	8.5	0	9.8	-0.3
Hs.208229	84634	<i>GPR54</i>	<i>G protein-coupled receptor 54</i>	7.9	-0.9	8.1	-0.8	8.4	0.2

NOTE: Total RNA was isolated from HUVEC following infection with either EGR-1-expressing adenoviruses or empty control viruses at 16, 24, and 48 hours. The RNA samples were subjected to microarray analysis using the Affymetrix U133 GeneChip set. Gene expression changes relative to noninfected control cultures for the EGR-1, and control viruses are displayed on a logarithmic scale (log 2). The full set of Affymetrix data is available in GEO database under ID GSE2299. A short list of the most highly up-regulated genes is available as Supplementary Table S2 from the authors on request.

preparations were done, and plaque-forming units (pfu) were determined in 293 cells as described (6). For infection, HUVEC were incubated in PBS for 30 minutes at multiplicities of infection of 100. Thereafter, cells were washed and cultured in normal HUVEC medium. Under these conditions, 100% of the HUVEC were infected as determined by GFP expression.

Real-time reverse transcription-PCR. RNA was extracted from cultured endothelial cells with Trizol (Invitrogen, Carlsbad, CA). Total RNA (2 μ g) was reverse transcribed into cDNA (SuperScript II RT, Invitrogen) using oligo(dT) primers, and real-time PCR was used to monitor gene expression using a LightCycler instrument (Hoffman-LaRoche, Basel, Switzerland) according to established procedures (11, 12). A list of the oligonucleotide primers used for gene amplification (Supplementary Table S1) can be obtained from the authors on request.

Western blots. Western blots were done as described by us previously (6). Total cell lysates in Laemmli buffer were separated by SDS-PAGE and transferred to Immobilon-P membranes (Millipore, Bedford, MA). The membranes were incubated with polyclonal anti-EGR-1, anti-VEGFR-1, or anti-Sp1 antibodies (Santa Cruz Biotechnology, Santa Cruz, CA) followed by horseradish peroxidase-labeled secondary antibodies (Amersham Life Sciences, Amersham Place, England). After washing, the membranes were incubated with enhanced chemiluminescence reagent (Amersham, Life Sciences).

Affymetrix microarray analysis. Preparation of cRNA, hybridization to the human U133 GeneChip set (Affymetrix, Santa Clara, CA), and scanning of the arrays were carried out according to the manufacturer's protocols¹ as described in more detail previously (13). Images were analyzed with GeneChip software (MAS 5.0, Affymetrix), and normalization was done by global scaling, with the arrays scaled to an average intensity of 500. Gene expression changes were calculated as the ratio of EGR-1- or control virus-infected cells to noninfected control cells. Genes were scored based on the putative biological functions of the encoded proteins, as determined by database searches using the NetAffx Gene Ontology Mining Tool¹ and a previously published classification scheme ("OntoExpress") for cellular functions (14). A full set of the Affymetrix data is available in the Gene Expression Omnibus (GEO) database (ID GSE2299), and a list of the 67 most highly up-regulated genes can be provided by the authors as Supplementary Table S2 on request.

In vitro tube formation and endothelial sprouting assays. The formation of capillary tube-like structures by HUVEC was analyzed on basement membrane matrix (Matrigel, Becton Dickinson, Franklin Lakes, NJ)

¹ <http://www.affymetrix.com>

as described (6). Cells were starved for 4 hours in M199 medium containing 1% SCS, seeded on Matrigel (3×10^4 cells per well), and further incubated for 16 hours. Images of the network were taken on a phase-contrast microscope (Nikon Diaphot TMD, Kawasaki, Japan) using a cooled charge-coupled device camera (Kappa DX30, Kappa GmbH, Gleichen, Germany). The length of the tube-like structures formed was determined with the AnalySiS software (Softimaging System, Munster, Germany). Endothelial sprouting was assessed by a modification of the method used by Nehls et al. (15) as described previously (6). Briefly, microcarrier beads (Cytodex 3, Sigma Chemical Co., St. Louis, MO) were seeded with HSMEC and embedded into fibrin gels with or without 50 ng/mL VEGF, 50 ng/mL bFGF, or both factors. After formation of the fibrin gels, cultures were incubated with additional M199 medium containing 20% FCS with or without growth factors. After 2 days, the number of tube-like sprouts formed/microcarrier bead was counted. Only sprouts of $\sim 150 \mu\text{m}$ were scored. To visualize cell nuclei, cells were fixed with 3.7% formaldehyde and 2% sucrose in PBS and permeabilized with 0.5% Triton X-100 in PBS. Hoechst 333258 (500 ng/mL) was then added for 30 minutes, and the cytoskeleton stained with rhodamine-phalloidin (Invitrogen) for 1 hour in the dark.

Murine Matrigel assay. Matrigel basement solution (Becton Dickinson) was supplemented with 1.5×10^8 pfu/mL recombinant adenoviruses and 300 ng/mL VEGF and injected s.c. into the flank region of female C57BL/6j mice (16). On day 6 after infection, the mice were sacrificed, and the Matrigel plug was removed and embedded in paraffin. Cryosections of the plug were prepared and stained with H&E (Merck, Darmstadt, Germany). Immunofluorescence was then done using rat anti-CD31 antibody, and nuclei were counterstained with 4',6-diamidino-2-phenylindole (DAPI; Vector Laboratories, Burlingame, CA) as described (16). Pictures were taken on an Olympus AX-70 microscope (Olympus Optical Co., Tokyo, Japan) using an F-View camera. The number of cells in the Matrigel plug was quantified on pictures displaying complete sections of the plug. The circular section images were divided into 10-degree segments, and the number of cells within six segments was counted for each section.

Murine fibrosarcoma model. MethA fibrosarcoma (10) cultures were harvested in exponential growth phase, and 1.5×10^6 cells in 50 μL PBS were injected s.c. into the dorsal skin of C57Bl/6j female mice (10). Following tumor formation (4 days after inoculation), tumors were given 5×10^8 pfu recombinant adenoviruses (Ad.GFP and Ad.EGR-1) diluted in 20 μL PBS, which was repeated after 2 days. Mice were sacrificed 3 days later, and tumor weights were determined. Frozen tumor sections (10 μm) were prepared for immunohistochemical analysis. Sections were then stained with either hematoxylin or immunofluorescence staining using rat anti-mouse VEGFR-2 (17), rat anti-mouse CD31, or rabbit anti-human EGR-1 antibodies (Santa Cruz) followed by incubation with Alexa Fluor 555-labeled anti-rabbit IgG, biotinylated goat anti-rat IgG, and Alexa Fluor 555- or Alexa Fluor 488-labeled streptavidin (Invitrogen). Nuclei were counterstained with DAPI. VEGFR-2, CD31, and EGR-1 staining was analyzed with an Olympus AX70 microscope. For quantification, six random microscopic fields representative of individual tumor sections were recorded with an F-View camera, and the fluorescent signals of VEGFR-2- or CD31-positive cells were quantified using AnalySiS Pro software.

Results and Discussion

In endothelial cells transduced with EGR-1-expressing adenoviruses, high EGR-1 mRNA and protein levels accumulated over the first 24 to 48 hours after infection and then remained constant for several days (Fig. 1A and B).

Based on preliminary data on the induction of repressive genes by EGR-1 and accompanying effects in angiogenesis assays, we established the repertoire of potential inhibitory genes induced by sustained EGR-1 expression using Affymetrix microarray analysis. The data revealed that 67 genes are up-regulated >30-fold 24 hours after infection (GEO database ID GSE2299). We have delineated several groups of up-regulated or down-regulated genes (Table 1), which are possibly directly related to the inhibitory effects

observed in angiogenesis models described below. The relative changes in mRNA levels for most of these genes were confirmed using quantitative real-time reverse transcription-PCR (RT-PCR; Fig. 1A, C, and E; data not shown).

We first confirmed the effects of sustained EGR-1 expression on described EGR-1 target genes, which have potential influence on angiogenesis. These experiments revealed that sustained EGR-1 expression induced VEGFR-1 (Flt-1) expression on the mRNA and protein level (Fig. 1C and D). Coinfections using NAB2 and NAB2.as adenoviruses revealed the specificity of EGR-1-mediated up-regulation (Fig. 1D). Whereas NAB2 inhibited EGR-1-mediated up-regulation (Fig. 1D, lane 6), a truncated nonrepressive variant NAB2.as (9) failed to show a similar effect (Fig. 1D, lane 7). In this context, it is important that several reports have shown that transmembrane and soluble forms of VEGFR-1 can counteract proangiogenic VEGFR-2 activity and function as decoy receptors (18, 19), although recent data also support a synergistic role of VEGFR-1 and VEGFR-2 in tumor angiogenesis (20). We also

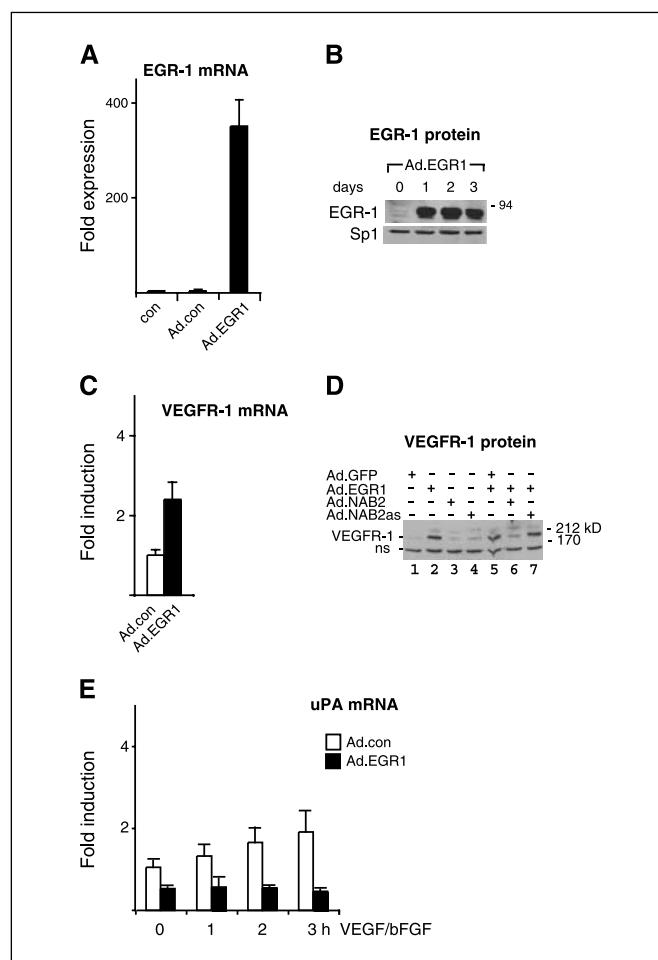


Figure 1. Effects of sustained EGR-1 expression in endothelial cells. HUVEC were infected with EGR-1 adenoviruses or control viruses for 24 hours or as indicated, and mRNA was isolated from uninduced samples or cultures induced with VEGF and bFGF for 1 to 3 hours and analyzed using real-time RT-PCR. EGR-1 and VEGFR-1 protein levels were determined by Western blotting in (B) and (D), respectively. A, EGR-1 mRNA and (B) EGR-1 protein produced from the EGR-1 adenovirus. C, up-regulation of VEGFR-1 mRNA by EGR-1 virus. D, up-regulation of VEGFR-1 protein by EGR-1 and inhibition by Ad.NAB2. NAB2.as, nonrepressive variant of NAB2. ns, unspecific band. E, loss of VEGF/bFGF inducibility of uPA mRNA through EGR-1 expression.

evaluated the influence of sustained EGR-1 expression on the induction of the proangiogenic *urokinase-type plasminogen activator* (*uPA*) gene (21), which is up-regulated by VEGF and bFGF (6). In contrast to VEGFR-1, *uPA* mRNA was reduced two-fold in EGR-1 virus compared with control virus-infected cells and was not induced by combined VEGF and bFGF stimulation (Fig. 1E).

In the microarray data (Table 1), we detected up-regulated genes with repressive functions on transcription, including not only NAB1 and NAB2, two specific corepressors of EGR-1 (9), but also JunB and JunD. JunB has been proposed to counteract the induction of cell cycle-promoting genes by activator protein 1 complexes by replacing c-Jun in the complex (22), and JunD has been shown to reduce tumor angiogenesis (23). Regulated genes with anti-proliferative activity also include two cell cycle check point effectors, p57/KIP2 (24) and GADD45B (25), as well as transforming growth factor- β (TGF- β ; ref. 26).

Importantly, we also detect several changes, which could interfere with specific processes essential for angiogenesis. The chemokine ligand BRAK/CXCL14, known to block endothelial chemotaxis and angiogenesis, was up-regulated by EGR-1 (27). In addition, both tissue inhibitor of metalloproteinase (TIMP)-1 and TIMP-3, which can inhibit the invasive potential of cells (28), were strongly induced. TIMP-3 also inhibits angiogenesis directly by blocking the binding of VEGF to VEGFR-2 (29). Potential anti-angiogenic effects triggered by sustained EGR-1 expression include a reduction of VEGFR-2 (KDR) message (Table 1).

A third group of regulated transcripts likely contributing to the antiangiogenic and antitumoral effects described below comprises several genes linked to the induction of apoptosis, such as *SIVA* (30), *DEDD2* (31), and *DUSP2* (32).

These data were in accordance with the hypothesis that sustained EGR-1 expression would shift the balance from activation to repressive feedback mechanisms in endothelial cells. We therefore investigated whether these effects on gene expression are reflected in angiogenesis assays. Indeed, when the ability of EGR-1 virus-infected HUVEC to migrate and form a tubular network on Matrigel was tested, we observed an almost complete inhibition of migration and tubule formation, whereas GFP control virus-infected cells formed normal tubular structures within 12 to 24 hours (Fig. 2A). When seeded on Matrigel, EGR-1 virus-infected cells undergo rapid apoptosis within 16 hours. This could be facilitated by the lack of survival signals in cells on Matrigel when stabilizing cell-cell contacts cannot be formed under conditions inhibitory for migration and tube formation. In accordance with this assumption, EGR-1 virus-infected cells seemed not affected after 24 hours when seeded on gelatin (Fig. 2A, bottom). However, apoptosis also became apparent in cells seeded on gelatin after 3 to 4 days (Fig. 2C), likely caused by the increased expression of proapoptotic genes as displayed in Table 1. Apoptotic cell death was confirmed by the presence of apoptotic bodies and DNA laddering assays (Fig. 2C).

Next, we analyzed the sprouting of microvascular endothelial cells into fibrin gels, which is dependent on VEGF or bFGF stimulation and the ability of cells to degrade and invade the three-dimensional gel following the formation of filopodia (6, 15). EGR-1-expressing cells almost completely lost the ability to form sprouts when triggered with VEGF (Fig. 2B), whereas GFP control virus-infected cells formed normal sprouts consisting of cells consecutively invading the fibrin gel. A similar inhibition by EGR-1 was observed when a mixture of VEGF and bFGF (Fig. 2B) was used to trigger sprout formation. Because both Matrigel tubule formation

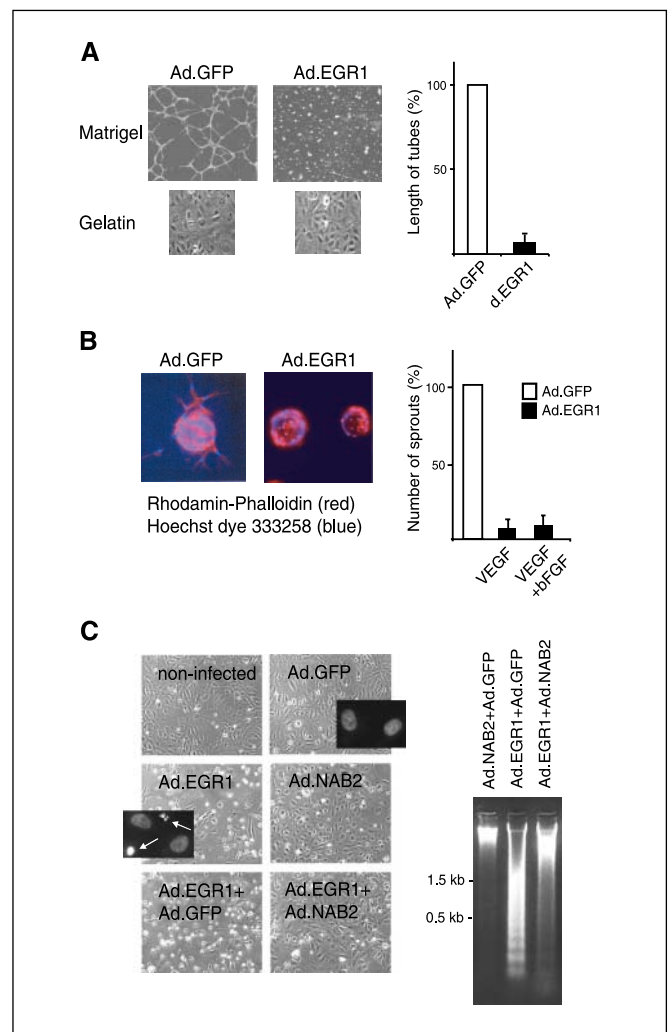


Figure 2. Inhibition of tubule and sprout formation in angiogenesis models *in vitro* and induction of apoptosis. **A**, *in vitro* Matrigel model: HUVEC were infected with EGR-1 and control GFP adenoviruses and seeded in parallel on either Matrigel- or gelatin-coated tissue culture plates 24 hours after infection. Sixteen hours thereafter, cultures were assessed by phase-contrast microscopy (top, Matrigel-coated plates; bottom, gelatin-coated plates). Right, the total length of tubules formed was measured. **B**, *in vitro* sprout formation assay in fibrin gels: HUVEC infected for 24 hours were seeded onto Cytodex beads, incubated overnight, and then incorporated into fibrin gels in the presence or absence of VEGF or a mixture of VEGF and bFGF. Left, after 48 hours, the cytoskeleton and nuclei were stained with rhodamine-phalloidin (red) and Hoechst dye 333258 (blue), respectively, and evaluated by phase-contrast microscopy; right, the numbers of sprouts were scored to quantitate percentage inhibition. Three independent experiments with duplicate samples were done for both assays. Columns, mean; bars, SD. **C**, apoptosis induction in EGR-1 virus-infected cells 72 hours after infection: HUVEC seeded on gelatin-coated plates were infected with the viruses. Left, 48 hours after infection, cells started to show increasing signs of apoptosis, such as formation of apoptotic bodies, which led to a reduction in cell number of >50% at 72 hours. Inset, arrow, the formation of apoptotic bodies was displayed by staining with Hoechst dye. Right, apoptotic cell death was confirmed by DNA laddering assays 72 hours after infection. Survival was partially restored by coinfection with Ad.NAB2.

and fibrin sprouting are largely independent of cell proliferation, it is likely that EGR-1 overexpression directly inhibited the ability of endothelial cells to migrate and/or form filopodia and tubular structures. The inability to form sprouts could have been caused by the decrease in the inducibility of proteases, such as *uPA*, or the increase in the synthesis of protease inhibitors, such as TIMP-1 and TIMP-3.

We next evaluated the effects of EGR-1 overexpression in the murine Matrigel plug model, a widely used model of angiogenesis *in vivo* (6, 16). When Matrigel plugs containing the control viruses and VEGF were injected s.c. into C57Bl/6J mice, a massive migration and invasion of cells and the formation of vessel-like structures were observed in the plug within 6 days (Fig. 3A and B). In contrast, when Ad.EGR-1 was mixed into the VEGF-supplemented Matrigel, no increased cell invasion was observed (Fig. 3B). Vessels were found solely in the cell layer formed regularly on the outside of the Matrigel plug. These results show that EGR-1 possesses a strong inhibitory capacity on the angiogenic activity of VEGF *in vivo*.

Finally, we tested the effect of the adenoviruses on the growth of preestablished fibrosarcomas in mice (Fig. 3C and D). Tumor lesions were injected on days 4 and 6 after implantation with the viruses and analyzed on day 8 or 9 similar as described previously (10). Treatment with EGR-1 virus reduced tumor weight by ~70% to 80% (Fig. 3D, top). When tumor sections were stained for VEGFR-2 expression, a strong and significant reduction in the levels of VEGFR-2 expression between 60% to 70% was observed (Fig. 3C, middle; Fig. 3D, bottom). This was much more pronounced than

the reduction in CD31 staining, which was reduced only 20% at the time points analyzed (data not shown). This suggests a changed functional state of vessels in the EGR-1 virus-injected tumors and that these contain significantly less growing neovessels because it has been shown that VEGFR-2 expression is a marker of actively growing tumor vessels (33). For control purposes, EGR-1 expression was confirmed in the analyzed regions by staining with an antibody against human EGR-1 (Fig. 3C, bottom). In EGR-1 virus-injected tumors, high EGR-1 expression could be detected in tumor cells (Fig. 3C) as well as CD31-positive endothelial cells (data not shown).

Based on the reduced VEGFR-2 staining and the very strong inhibition of *in vitro* and *in vivo* angiogenesis assays described in Fig. 2A and B and Fig. 3A and B, we assume that the reduction of tumor growth observed is at least in part due to inhibition of angiogenesis. It is possible that a direct inhibition of tumor cell proliferation, as suggested by the results of others (34), contributes to the effect. We have further preliminary evidence that different tumor cells infected with EGR-1 viruses up-regulate several of the genes identified in this study in endothelial cells, which could further contribute to inhibition of angiogenesis (e.g., by increased

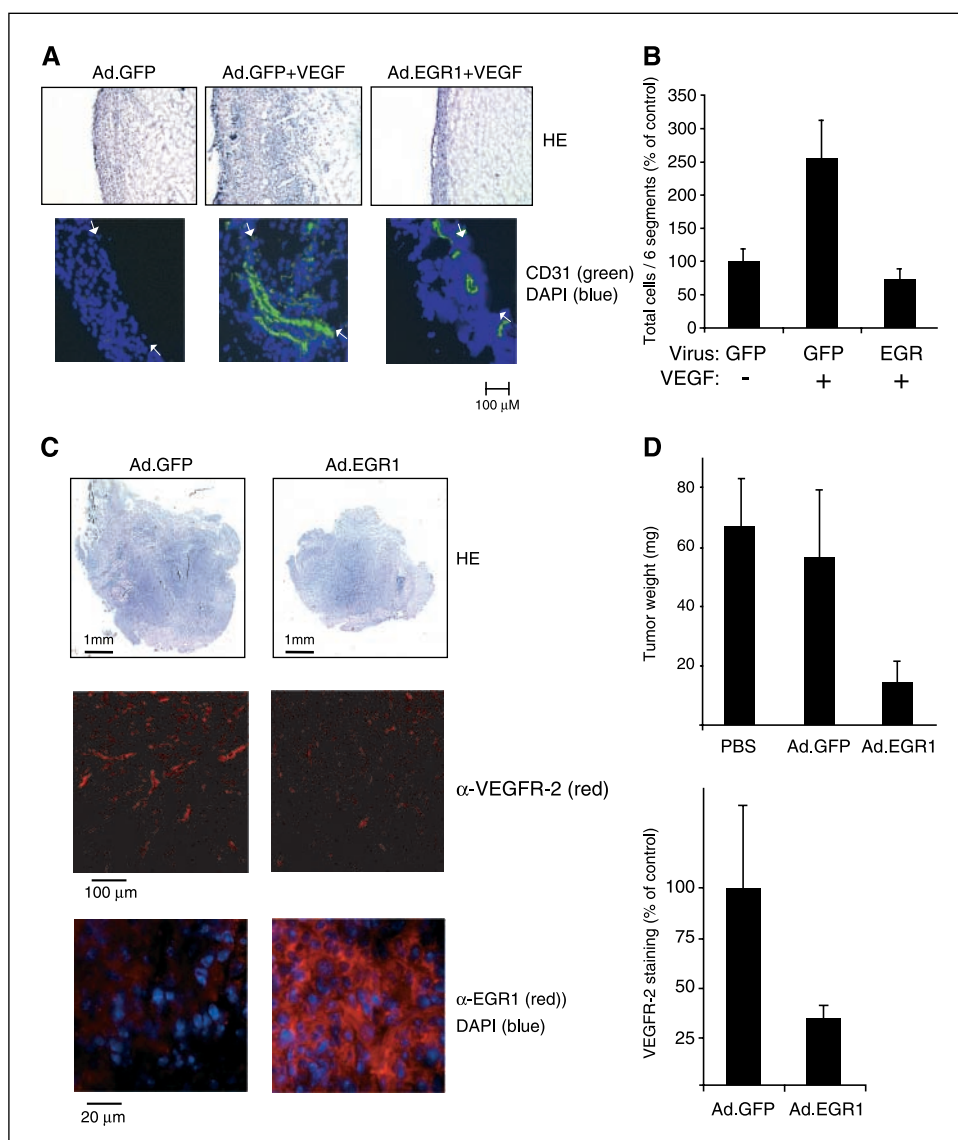


Figure 3. Inhibition of angiogenesis and tumor growth *in vivo*. *A*, murine Matrigel model: Ad.EGR-1 and Ad.GFP (1.5×10^8 pfu/mL) were added to Matrigel solution with or without addition of VEGF (300 ng/mL) and injected s.c. into mice. After 6 days, sections were prepared from the plugs and stained with H&E (HE; top) or with anti-CD31 antibodies and DAPI (bottom). Left to right, the images display the rim of cells regularly formed around the Matrigel plug followed by a section through the plug. Arrows, the border between the rim and the Matrigel. *B*, total cells in sections of the Matrigel plug were quantified as described in Materials and Methods. Columns, mean of two experiments in duplicates; bars, SD. *C*, murine fibrosarcoma model: MethA fibrosarcoma cells were injected s.c. into the back of C57Bl/6J mice. On day 4 and, again, on day 6, fibrosarcomas were inoculated with EGR-1 adenoviruses or control GFP viruses. On day 9, tumors were resected, tumor masses were determined, and sections were prepared for histochemical analysis. Cryosections were either stained with hematoxylin (top), rat anti-mouse VEGFR-2 (middle), or rabbit anti-human EGR-1 antibodies and DAPI (bottom). *D*, reductions in fibrosarcoma tumor weight (top) and VEGFR-2 staining (bottom). Columns, mean of three experiments with three animals per group; bars, SD. Fluorescence intensities of VEGFR-2 staining of individual sections of the tumors were measured as described in Materials and Methods.

TIMP production) or be involved in direct inhibition of growth and induction of apoptosis in tumor cells.

The data obtained are in accordance with the possibility that the genes described are up-regulated in a negative feedback loop to limit biological effects triggered by EGR-1 activity. EGR-1 is normally induced only transiently and in a balanced way in response to growth factors because prolonged and excessive activation of some of the genes induced by EGR-1 might otherwise be harmful to normal cells leading to uncontrolled responses. EGR-1 seems to be able to do two opposing functions: a proangiogenic after transient expression and an antiangiogenic, antiproliferative after sustained expression. In line with this suggestion, it has been recently shown that EGR-1 can induce or repress transcription of certain genes depending on the stimulus. These pleiotropic effects of EGR-1 are regulated by post-translational modification of EGR-1 (35). Whereas serum induction of EGR-1 leads to up-regulation of p300/CBP, acetylation of EGR-1, and induction of survival and growth genes, UV irradiation induces phosphorylation of EGR-1, which then triggers growth-inhibitory and proapoptotic responses (35). UV induction of EGR-1 also leads to more sustained production of EGR-1 over several hours when compared with the transient induction by growth factors (35). Similar to UV induction, it is possible that sustained overexpression of EGR-1 by adenoviruses leads to preferential production of EGR-1 forms, which function in inhibitory responses.

Based on the results described, we propose that gene therapy using EGR-1-expressing adenoviruses or nonviral vectors might constitute a new therapeutic principle to inhibit tumor angiogenesis and tumor growth. When delivered by direct injection into tumors, it can exert effects not only by interfering with several growth-promoting and survival pathways in the infected cells but also by inducing the secretion of a series of antiangiogenic molecules affecting neighboring cells. Furthermore, it could possibly be of advantage to apply viruses targeted to the tumor vasculature via the bloodstream, which are currently in development (36). It is conceivable that disseminated metastases could be targeted in this way. We believe that the prominent effects displayed warrant further evaluation to establish the therapeutic potential of sustained EGR-1 expression.

Acknowledgments

Received 8/2/2005; revised 4/13/2006; accepted 4/24/2006.

Grant support: Austrian Science Fund grant NFN-S94-3 and European Commission grant QLK3-2002-02059 (E. Hofer) and Marie Curie Intra-European Fellowships, MEIF-CT-2003-500034 (M. Lucerna).

The costs of publication of this article were defrayed in part by the payment of page charges. This article must therefore be hereby marked *advertisement* in accordance with 18 U.S.C. Section 1734 solely to indicate this fact.

We thank all the members of the Department for Vascular Biology, Medical University of Vienna (Vienna, Austria) for help and discussions throughout the work, Christa Rabeck for preparations of endothelial cells, and Drs. Trevor Lucas and Renate Hofer-Warbinek for corrections and suggestions on the article.

References

- Folkman J, Kalluri R. Cancer without disease. *Nature* 2004;427:787.
- Carmeliet P. Manipulating angiogenesis in medicine. *J Intern Med* 2004;255:538-61.
- Ferrara N. Vascular endothelial growth factor: basic science and clinical progress. *Endocr Rev* 2004;25:581-611.
- Gashler A, Sukhatme VP. Early growth response protein 1 (Egr-1): prototype of a zinc-finger family of transcription factors. *Prog Nucleic Acid Res Mol Biol* 1995;50:191-224.
- Fahmy RG, Dass CR, Sun LQ, Chesterman CN, Khachigian LM. Transcription factor Egr-1 supports FGF-dependent angiogenesis during neovascularization and tumor growth. *Nat Med* 2003;9:1026-32.
- Lucerna M, Mechtcheriakova D, Kadl A, et al. NAB2, a corepressor of EGR-1, inhibits vascular endothelial growth factor-mediated gene induction and angiogenic responses of endothelial cells. *J Biol Chem* 2003;278:11433-40.
- Yan SF, Fujita T, Lu J, et al. Egr-1, a master switch coordinating upregulation of divergent gene families underlying ischemic stress. *Nat Med* 2000;6:1355-61.
- Silverman ES, Collins T. Pathways of Egr-1-mediated gene transcription in vascular biology. *Am J Pathol* 1999;154:665-70.
- Svaren J, Severson BR, Apel ED, Zimonjic DB, Popescu NC, Milbrandt J. NAB2, a corepressor of NGFI-A (Egr-1) and Krox20, is induced by proliferative and differentiative stimuli. *Mol Cell Biol* 1996;16:3545-53.
- Heidenreich R, Machein M, Nicolaus A, et al. Inhibition of solid tumor growth by gene transfer of VEGF receptor-1 mutants. *Int J Cancer* 2004;111:348-57.
- Pfaffl MW. A new mathematical model for relative quantification in real-time RT-PCR. *Nucleic Acids Res* 2001;29:e45.
- Gruber F, Hufnagl P, Hofer-Warbinek R, et al. Direct binding of Nur77/NAK-1 to the plasminogen activator inhibitor 1 (PAI-1) promoter regulates TNF α induced PAI-1 expression. *Blood* 2003;101:3042-8.
- Bilban M, Ghaffari-Tabrizi N, Hintermann E, et al. Kisspeptin-10, a KiSS-1/metastatin-derived decapeptide, is a physiological invasion inhibitor of primary human trophoblasts. *J Cell Sci* 2004;117:1319-28.
- Khatri P, Draghici S, Ostermeier GC, Krawetz SA. Profiling gene expression using onto-express. *Genomics* 2002;79:266-70.
- Nehls V, Schuchardt E, Drenckhahn D. The effect of fibroblasts, vascular smooth muscle cells, and pericytes on sprout formation of endothelial cells in a fibrin gel angiogenesis system. *Microvasc Res* 1994;48:349-63.
- Passaniti A, Taylor RM, Pili R, et al. A simple, quantitative method for assessing angiogenesis and antiangiogenic agents using reconstituted basement membrane, heparin, and fibroblast growth factor. *Lab Invest* 1992;67:519-28.
- Kataoka H, Takakura N, Nishikawa S, et al. Expressions of PDGF receptor α , c-Kit, and Flk1 genes clustering in mouse chromosome 5 define distinct subsets of nascent mesodermal cells. *Dev Growth Differ* 1997;39:729-40.
- Hiratsuka S, Minowa O, Kuno J, Noda T, Shibuya M. Flt-1 lacking the tyrosine kinase domain is sufficient for normal development and angiogenesis in mice. *Proc Natl Acad Sci U S A* 1998;95:9349-54.
- Park JE, Chen HH, Winer J, Houck KA, Ferrara N. Placenta growth factor. Potentiation of vascular endothelial growth factor bioactivity, *in vitro* and *in vivo*, and high affinity binding to Flt-1 but not to Flk-1/KDR. *J Biol Chem* 1994;269:25646-54.
- Carmeliet P, Moons L, Lutun A, et al. Synergism between vascular endothelial growth factor and placental growth factor contributes to angiogenesis and plasma extravasation in pathological conditions. *Nat Med* 2001;7:575-83.
- Li H, Lu H, Griscelli F, et al. Adenovirus-mediated delivery of a uPA/uPAR antagonist suppresses angiogenesis-dependent tumor growth and dissemination in mice. *Gene Ther* 1998;5:1105-13.
- Eferl R, Wagner EF. AP-1: a double-edged sword in tumorigenesis. *Nat Rev Cancer* 2003;3:859-68.
- Gerald D, Berra E, Frapart YM, et al. JunD reduces tumor angiogenesis by protecting cells from oxidative stress. *Cell* 2004;118:781-94.
- Yang HY, Shao R, Hung MC, Lee MH. p27 Kip1 inhibits HER2/neu-mediated cell growth and tumorigenesis. *Oncogene* 2001;20:3695-702.
- Thyss R, Virolle V, Imbert V, Peyron JF, Aberdam D, Virolle T. NF- κ B/Egr-1/Gadd45 are sequentially activated upon UVB irradiation to mediate epidermal cell death. *EMBO J* 2005;24:128-37.
- Sutton AB, Canfield AE, Schor SL, Grant ME, Schor AM. The response of endothelial cells to TGF β -1 is dependent upon cell shape, proliferative state, and the nature of the substratum. *J Cell Sci* 1991;99:777-87.
- Shellenberger TD, Wang M, Gujrati M, et al. BRAK/CXCL14 is a potent inhibitor of angiogenesis and a chemotactic factor for immature dendritic cells. *Cancer Res* 2004;64:8262-70.
- Rigg AS, Lemoine NR. Adenoviral delivery of TIMP1 or TIMP2 can modify the invasive behavior of pancreatic cancer and can have a significant antitumor effect *in vivo*. *Cancer Gene Ther* 2001;8:869-78.
- Qi JH, Ebrahem Q, Moore N, et al. A novel function for tissue inhibitor of metalloproteinases-3 (TIMP3): inhibition of angiogenesis by blockage of VEGF binding to VEGF receptor-2. *Nat Med* 2003;9:407-15.
- Fortin A, MacLaurin JG, Arbour N, et al. The proapoptotic gene SIVA is a direct transcriptional target for the tumor suppressors p53 and E2F1. *J Biol Chem* 2004;279:28706-14.
- Alcivar A, Hu S, Tang J, Yang X. DEDD and DEDD2 associate with caspase-8/10 and signal cell death. *Oncogene* 2003;22:291-7.
- Yin Y, Liu YX, Jin YJ, Hall EJ, Barrett JC. PAC1 phosphatase is a transcription target of p53 in signalling apoptosis and growth suppression. *Nature* 2003;422:527-31.
- Vajkoczy P, Farhadi M, Gaumann A, et al. Microtumor growth initiates angiogenic sprouting with simultaneous expression of VEGF, VEGF receptor-2, and angiopoietin-2. *J Clin Invest* 2002;109:777-85.
- Calogero A, Lombardi V, De Gregorio G, et al. Inhibition of cell growth by EGR-1 in human primary cultures from malignant glioma. *Cancer Cell Int* 2004;4:1.
- Yu J, de Belle I, Liang H, Adamson ED. Coactivating factors p300 and CBP are transcriptionally crossregulated by Egr1 in prostate cells, leading to divergent responses. *Mol Cell* 2004;15:83-94.
- Ogawara K, Rots MG, Kok RJ, et al. A novel strategy to modify adenovirus tropism and enhance transgene delivery to activated vascular endothelial cells *in vitro* and *in vivo*. *Hum Gene Ther* 2004;15:433-43.